

# Overview of Human-Machine Coupling Mechanism Design for Knee Exoskeletons

Xu Huang<sup>1</sup>, Xudong Yu<sup>2,\*</sup>

<sup>1</sup>School of Health Science and Engineering, University of Shanghai for Science and Technology, Shanghai, China

<sup>2</sup>PLA Naval Medical Center, Naval Medical University, Shanghai, China

\*Corresponding author: yuxudongtoyou@263.net

**Abstract:** The knee exoskeleton is gradually becoming an essential component in people's daily lives, playing a significant role in the fields of rehabilitation and industry. However, the human-machine coupling issue remains a key factor affecting exoskeleton performance. Therefore, this paper provides an overview of the design of the human-machine coupling mechanism for knee exoskeletons. In terms of structural design, the mechanisms are categorized into the simplified fixed-track mechanism, the compliant elastic mechanism, and the self-calibration mechanism, with an analysis of their performance in practical applications. Moreover, this paper discusses the general optimization steps of optimization algorithms and their applications in mechanism optimization. Finally, the challenges currently faced by knee exoskeletons are summarized, and future prospects are proposed.

**Keywords:** Knee Exoskeleton; Human-Machine Coupling Mechanism; Mechanism Optimization

## 1. Introduction

As a wearable device, exoskeletons can not only assist healthy individuals in reducing energy consumption but also provide support for patients with mobility impairments. With the acceleration of global aging and the increasing demand for health and physical assistance, exoskeletons have shown great potential in rehabilitation and have gradually been applied in various fields, including assisting the elderly in daily activities, improving work efficiency, and enhancing athletic performance<sup>[1-3]</sup>. To meet the needs of different applications, various types of exoskeleton robots have been developed to assist the movement of the neck, upper limbs, lower back, hip, knee, and ankle joints<sup>[4-8]</sup>. However, the knee joint, as one of the most complex and vulnerable joints in the human body, bears body weight during walking, running, and sitting while absorbing impact forces<sup>[9]</sup>. Moreover, the incidence of diseases such as osteoarthritis increases with age<sup>[10]</sup>. Therefore, reducing the internal forces of the knee joint and improving mobility in daily life remain key research challenges.

Despite significant advancements in exoskeleton control and actuation technologies, the human-exoskeleton interaction remains poorly optimized, posing a major barrier to performance enhancement and long-term application<sup>[11]</sup>. To meet the personalized needs of users, designing an ergonomically compliant knee exoskeleton is of great importance. Therefore, this paper primarily focuses on the design and optimization of human-machine coupling mechanisms for knee exoskeleton.

## 2. Physiological structure of the knee joint

The knee joint (Figure 1) is composed of the lower end of the femur, the upper end of the tibia, the patella, the menisci, the anterior cruciate ligament (ACL), the posterior cruciate ligament (PCL), the medial collateral ligament (MCL), and the lateral collateral ligament (LCL). The MCL and LCL restrict lateral movements of the knee, while the ACL and PCL limit anterior-posterior motions. These ligaments influence the percentage of the rolling-to-sliding ratio in the knee joint. Additionally, the distinct shapes of the medial and lateral femoral condyles induce internal rotation during knee flexion. The lateral and medial menisci distribute weight over a larger area, protect the articular cartilage, and assist in stabilizing the knee by supporting the ligaments.

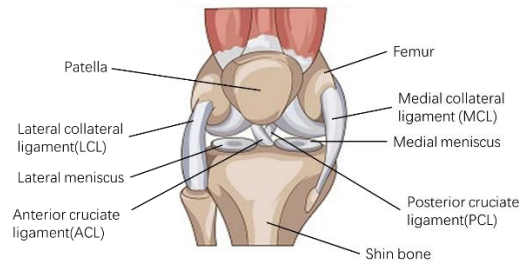


Figure 1: Schematic diagram of the knee joint.

According to the anatomical structure of the human lower limb, knee joint motion encompasses flexion and extension in the sagittal plane, internal and external rotation in the horizontal plane, as well as varus and valgus movements in the coronal plane. The primary movement of the knee joint is flexion/extension, with a maximum flexion range of  $130^{\circ}$  to  $150^{\circ}$ . The valgus and varus angles of each individual's knee are fixed, with an approximate range of  $5^{\circ}$  to  $10^{\circ}$ <sup>[12,13]</sup>. According to the analysis of human physiological characteristics and biomechanical structure, when the femur moves relative to the tibia, it exhibits continuous Euler rotation and translation, which can be approximated by an elliptical trajectory highly similar to the shape of the femoral condyles in the sagittal plane<sup>[14]</sup>. This results in a misalignment between the instantaneous centers of rotation (ICR) of the human joint and the device joint, which may pose a potential risk to joint health. As shown in Figure 2, the movement of the knee joint ICR in space can be described by five parameters: flexion angle ( $\phi$ ), valgus angle ( $V$ ), internal rotation angle ( $R$ ), anterior-posterior translation ( $Z_{DIS}$ ), and superior-inferior translation ( $Y_{DIS}$ )<sup>[15]</sup>. Here,  $L$  and  $M$  represent the initial positions of the lateral and medial femoral condyle centers, respectively, while  $L'$  and  $M'$  denote the positions of these centers after a change in  $\phi$ .

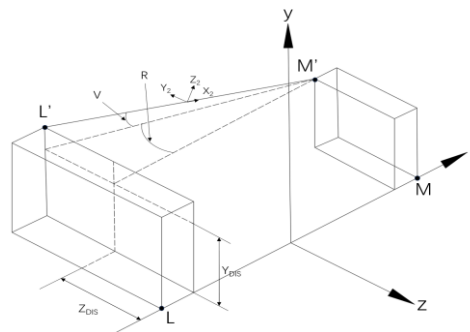


Figure 2: Schematic illustration of knee joint movement.

### 3. Design of knee exoskeleton mechanism

The initial rotation and subsequent sliding movement of the knee joint primarily occur in the sagittal plane [9]. When the human knee joint transitions from a static walking posture to a dynamic posture, the relative sliding between the femur and tibia is most pronounced, which can significantly reduce the efficiency of exoskeleton assistance<sup>[16,17]</sup>. If the robotic mechanism does not strictly follow the ICR of the knee joint, additional forces will be generated in the robotic fasteners. These potential tangential forces cause movement and sliding in the fastener positions, reducing the robot's service life<sup>[14]</sup>. Therefore, one of the key features of the knee joint mechanism is to follow the ICR of the knee joint. In some knee exoskeleton designs<sup>[18,19]</sup>, researchers have simplified the human knee joint as a 1-degree-of-freedom (DOF) rotational joint. Such oversimplified designs inevitably lead to misalignment of the human joint rotation axis, which may cause unwanted torques on the exoskeleton when worn, resulting in human discomfort, pain, or even injury<sup>[20]</sup>. According to the findings of reference<sup>[21]</sup>, over 77% of knee joint assistive devices do not consider alignment in their DOF design. Approximately 11% and 4% respectively employ single-DOF mechanisms and underactuated mechanisms, while only 8% use other mechanisms to achieve knee joint alignment.

#### 3.1. Simplified guidance mechanism

Simplified tracking mechanisms use multiple predefined trajectory coordinates or fitted trajectories to mimic the movement of the human knee joint, with data primarily derived from anatomical studies of

the knee joint's ICR, such as those by Shiraishi<sup>[22]</sup> and Walker<sup>[23]</sup>.

The four-bar (4-BM) mechanism is commonly used to replicate knee joint ICR motion and is one of the earliest knee mechanisms employed in prosthetics<sup>[24]</sup>. The 4-BM is used to simulate various aspects of the knee joint, including the ACL and PCL ligaments<sup>[25]</sup>, condylar shapes<sup>[26]</sup>, and the knee joint's center and axis<sup>[27]</sup>. Zhang et al<sup>[17]</sup> proposed a compliant knee exoskeleton based on the 4-BM, incorporating a spring-loaded cross 4-BM mechanism (Fig. 3a). The optimized design with the cross 4-BM and parallel springs reduced knee angle error, joint misalignment, and unintended interaction forces by  $16.5 \pm 1.3\%$ ,  $23.3 \pm 4.9\%$ , and  $17.7 \pm 1.3\%$ , respectively, compared to commercial products, while utilizing elastic potential energy recovery for gravity compensation.

Asker et al<sup>[28]</sup> introduced a knee joint structure based on a five-bar (5-BM) mechanism (Fig. 3b), where the optimized 5-BM produced a maximum ICR error 0.63 mm smaller than that of the 4-BM and demonstrated better force transmission capabilities.

In the case of six-bar mechanisms (6-BM), typical examples include the Watt<sup>[29]</sup> (Fig. 3c) and Stephenson III<sup>[30]</sup> (Fig. 3d) six-link mechanisms. Xiao et al<sup>[31]</sup> decomposed the Watt six-bar mechanism into trajectory-fitting 4-BM and drive 4-BM, comparing the linkage-driven 6-BM and crank-driven 6-BM. The results indicated that the crank-driven six-bar mechanism performed better in smoothing knee torque curves and transmission efficiency.

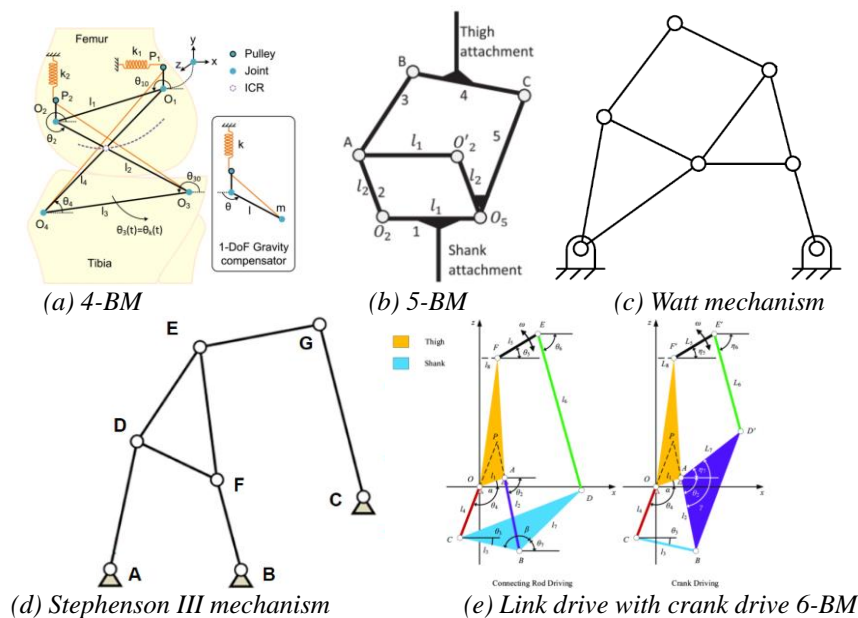


Figure 3: Design of Knee Joint Structure Based on Connecting Rod.

Increasing accuracy by adding linkages inevitably leads to greater structural complexity and inertia. To achieve more complex motion trajectories, researchers have incorporated gears or cams into the linkages.

Sabzali et al<sup>[32]</sup> proposed a novel non-circular gear four-bar (NGF) mechanism (Fig. 4a), which optimized the mechanism design through motion capture of the ICR, enabling precise tracking of knee joint movement and reducing actuator torque range and mechanism weight in dynamic optimization.

To address the complex problem of position synthesis, scholars designed a single-stage non-circular gear five-bar mechanism<sup>[33-35]</sup> (Fig. 4b), which consists of a single-stage non-circular gear system and a five-bar mechanism, offering smooth motion and overcoming the limitations found in traditional linkage mechanisms within their feasible solution domain.

For cam mechanism (CAM) design, the motion trajectory of the ICR is primarily used to determine the cam profile shape<sup>[36]</sup>. Omid et al<sup>[37]</sup> combined CAM with a spring assembly (SA) (Fig. 4c), designing the cam groove path based on the ICR on the sagittal plane to simulate the rotational and sliding motion of the human knee during the transition from sitting to standing. Compared to a single-degree-of-freedom rotational joint, the proposed knee joint mechanism reduced misalignment by 51%.

Soong et al<sup>[38]</sup> proposed a cam-gear mechanism consisting of a driven cam and a basic planetary gear system (Fig. 4d), which transmits and converts power. This mechanism offers advantages in generating

diversified continuous curved paths and symmetrical intersecting curved paths.

Kim et al<sup>[39]</sup>. integrated curved guides and bearings in their exoskeleton (Fig. 4e), and compared to traditional single-rotational joints, this biomimetic joint exhibited only 70% of the pressure differential, providing a certain advantage in reducing wearer discomfort.

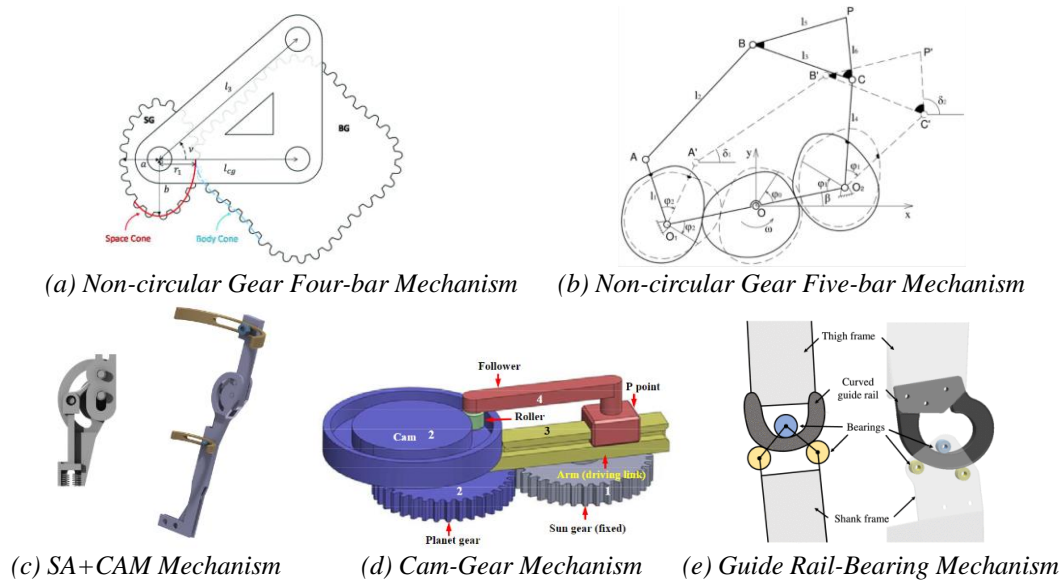


Figure 4: Composite Mechanism Based on Linkages.

Although a fixed trajectory simulates the average ICR curve, it fails to accommodate individual gait variations, such as step length and internal-external rotation angles. The ICR exhibits complex three-dimensional helical motion during the gait cycle, and rigid trajectories may lead to abnormal stress distribution on joint cartilage to varying degrees across different populations.

### 3.2. Compliant Elastic Mechanism

Elastic compliance mechanisms address the misalignment caused by lower limb flexion through the use of elastic or flexible components. Commonly, elastic components leverage the elastic displacement of variable stiffness materials to compensate for human-machine misalignment.

Liu et al<sup>[40]</sup>. designed two elastic limiters inspired by the cruciate ligament (Figure 5a), composed mainly of a guide rail, spring, bearing, and stopper. Pressure tests revealed that the exoskeleton reduced human-machine interaction forces by 50.9% during assisted walking and significantly decreased leg muscle activity under high-torque control for uphill walking.

Wang et al<sup>[41]</sup>. proposed a cross-shaped, four-degree-of-freedom mechanism (Figure 5b), where redundant degrees of freedom were constrained by springs, enhancing exoskeleton adaptability, dynamic performance, and user comfort while reducing mechanical complexity.

Zhao et al<sup>[42]</sup>. integrated elastic movable pairs into a four-bar mechanism to achieve variable stiffness (Figure 5c). This mechanism supports the positive load between the femur and tibia during the stance phase, reducing internal knee joint forces. Simulations showed that this design could bear 63.93% of the knee joint load during the stance phase.

Yang et al<sup>[43]</sup>. used polylactic acid (PLA) as an elastic knee joint component (Figure 5d), which provided substantial load support during standing and underwent elastic deformation during joint flexion. Experimental results showed that the exoskeleton reduced the load on one side of the knee joint by 110 N.



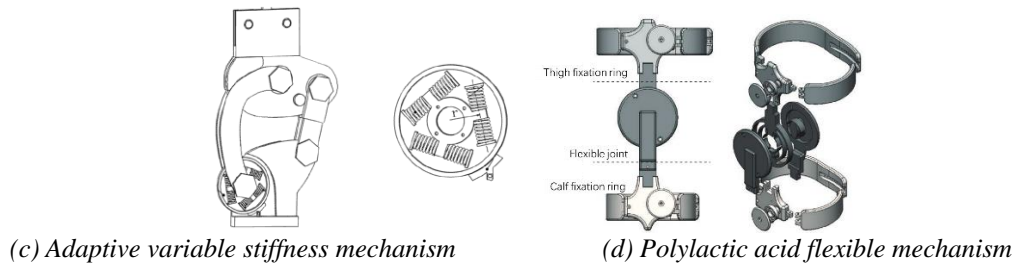


Figure 5: Compliance mechanism based on elastic components.

Flexible components primarily consist of airbags and fabrics. Wang et al. [59] developed a novel modular soft-rigid pneumatic exoskeleton (Figure 6a) that combines soft hinges with rigid links for better human conformation. The knee joint, acting as a soft hinge, is driven by a bidirectional curling pneumatic artificial muscle (CPAM), providing 28 Nm of torque with a maximum tracking error of 7.4°. The soft hinge design enhances comfort and flexibility while maintaining motion control throughout the gait cycle.

Sridar et al<sup>[44]</sup>. proposed a soft inflatable suit for knee extension in stroke rehabilitation (Figure 6b), composed of soft pneumatic actuators and an elastic sleeve supported by neoprene. By integrating an inertial measurement unit (IMU) and smart insole sensors for real-time knee angle and gait phase detection, along with a dual-layer control algorithm based on knee stiffness models, the exoskeleton reduced quadriceps activity by 30.06% to 57.16%.

Fang et al<sup>[45]</sup>. designed a novel foldable pneumatic bending structure inspired by an accordion bellow (Figure 6c), made from thermoplastic polyurethane (TPU) fabric. By inflating or compressing interconnected air chambers, the structure generated torque linearly with internal pressure and angle, producing up to 25.74 Nm of torque at 30° and 40 kPa. It could also output 21.80 Nm of torque without an external air source, reducing quadriceps electromyography (EMG) signals by up to 64.21%.

Panizzolo et al<sup>[46]</sup>. (Figure 6d) and Natali et al<sup>[47]</sup>. (Figure 6e) employed Bowden cables as the driving source in fabric-based soft suits made of Lycra and polyester webbing. Natali's design further incorporated elastic bands and an electromagnetic clutch for energy storage and release, optimizing energy efficiency. These designs reduced participants' net metabolic power by 7.3% to 14.2%, enhancing comfort and flexibility while minimizing reliance on traditional rigid exoskeletons.

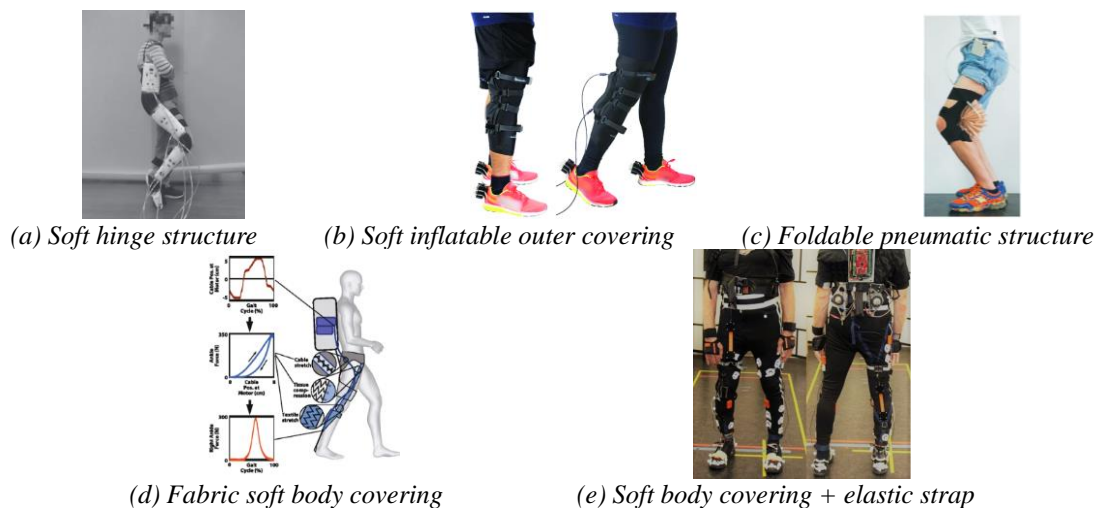


Figure 6: Compliance mechanism based on flexible components.

Although elastic compliance mechanisms have some adjustment capabilities for human-machine axis alignment, the nonlinear stiffness characteristics of elastic materials may lead to phase delay in human-machine interaction forces, especially during high-frequency movements, which can induce oscillations. Additionally, the parasitic forces generated by the attachment of elastic materials to the human body can cause varying degrees of discomfort. Therefore, the comfort of wearing such mechanisms may differ across individuals and requires further investigation. Improper elastic compensation could also increase metabolic costs, as muscles need to perform additional work to counteract the passive resistance of the elastic components.



### 3.3. Self-calibrating mechanism

Self-calibration mechanisms often incorporate the concept of kinematic redundancy to increase passive degrees of freedom (pDOF) and compensate for joint axis misalignment. Celebi et al<sup>[48]</sup>. proposed a lightweight mechanical structure based on a Schmidt coupling mechanism (Figure 7a), consisting of an input ring, an intermediate ring, an output ring, and multiple connecting links. It achieves knee flexion and anterior-posterior translation compensation through an active rotational degree of freedom driven by a Bowden-cable-based series elastic actuator and two passive translational degrees of freedom. This design achieves continuous torque output of up to 35.5 N m within a 180 ° rotation range, with a translational resolution of less than 0.05 mm and a rotational resolution of 0.2 °, demonstrating excellent force control performance and safety.

Choi et al<sup>[49]</sup>. proposed a self-aligning knee mechanism composed of a drive pulley, three alignment pulleys, two alignment links, two transmission cables, and thigh and shank connection frames (Figure 7b). By introducing two passive degrees of freedom (2-DoF), it compensates for the shift in the knee joint's rotation center during flexion and achieves a maximum rotation of 160 °.

Sarkisian et al<sup>[50]</sup>. designed a self-calibration mechanism based on a "Prismatic-Rotational-Rotational" (PRR) configuration (Figure 7c), which includes three passive degrees of freedom (pDOF). During sit-to-stand assistance, even with intentional alignment errors, the exoskeleton's peak unexpected force and torque were limited to below 5 N and 0.5 N m, respectively. The mechanism weighs only 190 g and can withstand knee torques up to 120 N m.

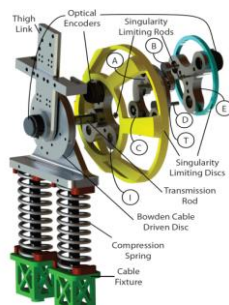
Yang et al<sup>[51]</sup>. introduced a human-machine wearable parallel (HMWP) mechanism (Figure 7d), similar to the design in<sup>[42]</sup>. It incorporates two additional degrees of freedom, including a sliding rail unit and a passive compensation unit. These components work in coordination to correct alignment errors caused by slippage during movement, individual knee geometry differences, axial motion, and wear at different positions.

Li et al<sup>[52]</sup>. designed a mechanism in the coronal plane (Figure 7e), consisting of a universal joint, a rotational joint, and two sliding joints. The rotational and sliding joints are passive, while the universal joint is actively driven via a Bowden cable transmission system. Compared to traditional single-DoF joints, this design reduced human-machine interaction force and torque by 28.1% and 72.1%, respectively.

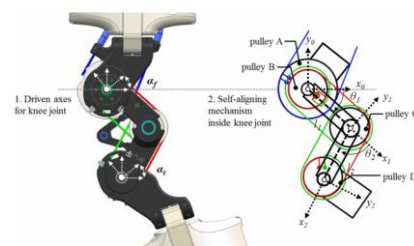
Choi et al<sup>[53]</sup>. developed a 3-DoF structure composed of a rolling joint, two passive alignment joints, a four-bar mechanism, and a sliding mechanism (Figure 7f). The two passive degrees of freedom are used for alignment in the coronal and sagittal planes, while the sliding mechanism and four-bar linkage transmit motor torque to the rolling joint for knee flexion. Despite reaching a torque assistance of 57.9 N m, the design reduced the wearer's metabolic cost by 1.03% to 1.17%.

Li et al<sup>[54]</sup>. employed a constant-force suspension mechanism and an adaptive compliant joint design (Figure 7g), with one active DoF and two passive DoFs. The rolling pair aligns with the instantaneous rotation center of the human knee, while the sliding pair automatically adjusts to wearing deviations and relative motion. With the constant-force suspension mechanism isolating impact from the load-bearing components, it reduced metabolic cost by 10.95%  $\pm$  4.40% during walking at 5 km/h and by 1.71%  $\pm$  4.54% during running at 9 km/h.

Yang et al<sup>[55]</sup>. proposed a multi-DoF adaptive structure based on a gear-linkage mechanism (Figure 7h), consisting of an active drive unit, gears, links, and passive hinge points. With one active DoF for flexion and two passive DoFs, this design introduced the Wearable Area (WA) metric, expanding alignment from "point-to-point" to "surface-to-point," achieving superior motion compatibility in terms of transmission ratio and initial stiffness.



(a) Schmidt coupling mechanism



(b) Cable-driven pulley mechanism

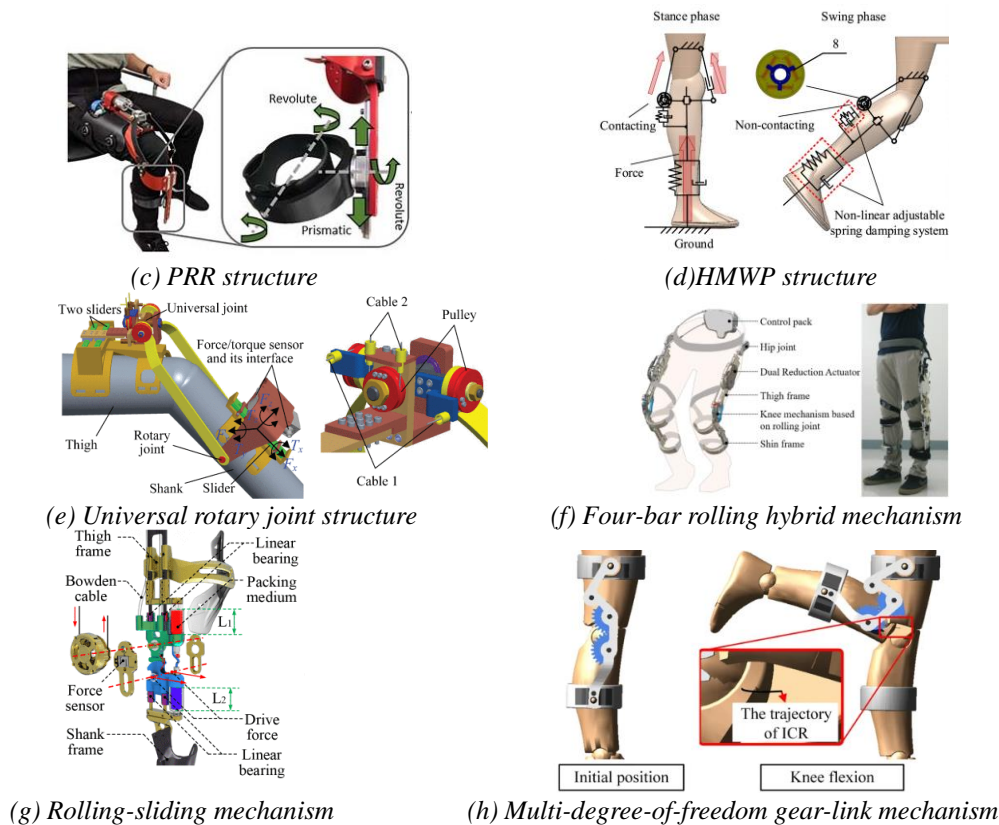


Figure 7: Self-calibrating mechanism.

Redundant degrees of freedom can reduce the intrinsic stiffness of the structure, so they are more commonly used with elastic actuators to balance compliance and support. For rigid adaptive structures, most are only available for sagittal or coronal planes, while the ability to adapt to complex 3D motions needs further verification.

#### 4. Parameter optimization and objective optimization methods

Mechanism optimization of knee exoskeletons is a crucial step in the design process, with the goal of improving the performance, comfort, and control accuracy of the exoskeleton by optimizing the structure and parameters of the knee actuation mechanism. In the design of related mechanisms, optimization methods usually involve the improvement of several aspects such as joint kinematics, dynamics, and load transfer paths. Choosing appropriate optimization methods can effectively deal with the complex constraints and nonlinear problems in the design, so as to improve the design efficiency and comfort while ensuring the mechanical performance.

Common parameter optimization methods include Multi-Objective Genetic Algorithm (MOGA), Multi-Objective Particle Swarm Optimization (MOPSO), Multi-Objective Differential Evolution (MODE), Weighted Sum Method (WSM), Pareto Local Search (PLS), Levenberg-Marquardt Algorithm Geometric Differentiation (GD), Goal Attainment Method (GAM) Nelder-Mead Simplex Method (NMSM), Interior Point Algorithm (IPA), Deep Neural Network Optimization (DNNO), Teaching-Learning-Based Optimization (TLBO), etc. Parametric optimization and multi-objective optimization method is mainly through the construction of one or more objective functions, the weight, stiffness, comfort, energy consumption and other comprehensive consideration, and then find a set of optimal parameters, so that the performance indicators to achieve a balance. The generic optimization steps are shown in Fig. 8. For example, the researcher<sup>[56]</sup> constructed a wear comfort evaluation function containing the maximum wear effective stress, soft tissue effective deformation and effective force node ratio, and through multi-objective genetic algorithm optimization, finally realized the exoskeleton to reduce the peak force and improve the soft tissue deformation during the walking process, which greatly improved the wear comfort. The researcher<sup>[57]</sup> determined the optimal link length and joint angle using SQP multi-objective optimization method by establishing a human spatial robotic coordinate system and introducing constraints such as overlapping self-interference and rotational collision, thus enabling the

exoskeleton to work in better coordination with the human body.

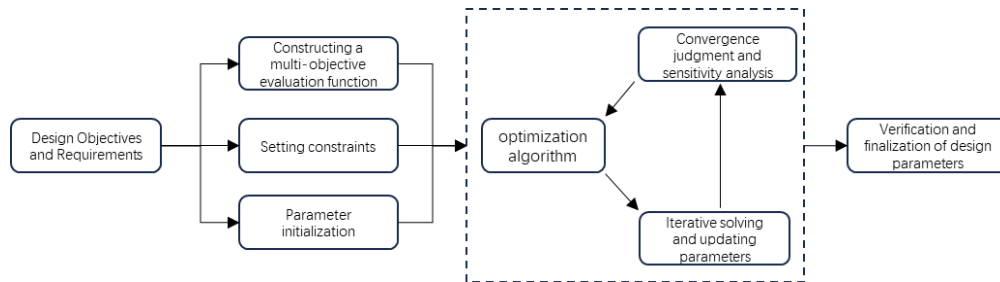


Figure 8: Generic Mechanism Optimization Procedure.

## 5. Conclusion and prospects

### 5.1. Conclusion

The structure of the human-machine coupling is a significant indicator of the knee exoskeleton, which not only affects the suitability of the exoskeleton when worn by a person, but may even affect the efficacy of rehabilitation therapy. Despite the significant advancements in control technology in recent years, the comfort of the exoskeleton remains a determining factor in an individual's decision to utilise it. Achieving an organic integration between the wearer and the exoskeleton, whilst simultaneously minimising discomfort, is imperative to ensure the optimal functionality of the exoskeleton in terms of both assistance and rehabilitation.

### 5.2. Prospects

The rapid development of robotics has led to the increasing use of exoskeletons in medical rehabilitation, daily life, and military applications. However, numerous challenges may arise in practical implementations. Human-machine compatibility is a critical issue for all types of exoskeletons. Although exoskeletons can transfer the workload to the core muscle tissues, prolonged use may lead to potential musculoskeletal disorders. Misalignment between the kinematics of the exoskeleton and human anatomy can increase cognitive load, meaning the wearer may consciously focus on the exoskeleton and its tasks. This increased cognitive load can negatively impact posture control.

From a mechanical design perspective, exoskeletons should possess characteristics such as high flexibility, wearability, strong adaptability, modularity, and lightweight construction. However, single-degree-of-freedom knee exoskeletons are unable to meet the complex motion requirements of the knee joint in three-dimensional space. With advances in soft materials for efficient force transmission, soft exoskeletons made from fabrics or elastomeric materials have been realized. These exoskeletons wrap around the body and work in parallel with muscles, significantly reducing the overall system mass. However, soft exoskeletons are still primarily in the experimental stage, with many challenges regarding stability and control accuracy. It is believed that in the near future, knee exoskeletons based on optimized human-machine coupling mechanisms will significantly contribute to the medical and industrial fields.

## References

- [1] Baronchelli F, Zucchella C, Serrao M, et al. The effect of robotic assisted gait training with Lokomat® on balance control after stroke: systematic review and meta-analysis[J]. *Frontiers in neurology*, 2021, 12: 661815.
- [2] Toedtheide A, Chen X, Sadeghian H, et al. A force-sensitive exoskeleton for teleoperation: An application in elderly care robotics[C]//2023 IEEE International Conference on Robotics and Automation (ICRA). IEEE, 2023: 12624-12630.
- [3] Cai M, Ji Z, Li Q, et al. Safety evaluation of human-robot collaboration for industrial exoskeleton[J]. *Safety science*, 2023, 164.
- [4] Garosi E, Mazloumi A, Jafari A H, et al. Design and ergonomic assessment of a passive head/neck supporting exoskeleton for overhead work use[J]. *Applied Ergonomics*, 2022, 101: 103699.
- [5] Gull M A, Bai S, Bak T. A review on design of upper limb exoskeletons[J]. *Robotics*, 2020, 9(1): 16.
- [6] Ji X, Wang D, Li P, et al. SIAT-WEXv2: A Wearable Exoskeleton for Reducing Lumbar Load during



*Lifting Tasks*[J]. *Complexity*, 2020, 2020: 1-12.

[7] Murray S A, Ha K H, Hartigan C, et al. An assistive control approach for a lower-limb exoskeleton to facilitate recovery of walking following stroke[J]. *IEEE transactions on neural systems and rehabilitation engineering*, 2014, 23(3): 441-449.

[8] Lee H, Ferguson P W, Rosen J. Lower limb exoskeleton systems—overview[J]. *Wearable Robotics*, 2020: 207-229.

[9] Wang D, Lee K M, Guo J, et al. Adaptive knee joint exoskeleton based on biological geometries[J]. *IEEE/ASME Transactions on Mechatronics*, 2013, 19(4): 1268-1278.

[10] Ibarra L G, Segura V H, Chávez D, et al. Las enfermedades y traumatismos del sistema músculo esquelético[J]. *Un análisis del Instituto Nacional de Rehabilitación de México, como base para su clasificación y prevención*, México, Secretaría de Salud, 2013: 147.

[11] Rupal B S, Rafique S, Singla A, et al. Lower-limb exoskeletons: Research trends and regulatory guidelines in medical and non-medical applications[J]. *International Journal of Advanced Robotic Systems*, 2017, 14(6).

[12] Lee K M, Guo J. Kinematic and dynamic analysis of an anatomically based knee joint[J]. *Journal of biomechanics*, 2010, 43(7): 1231-1236.

[13] Wismans J A C, Veldpaus F, Janssen J, et al. A three-dimensional mathematical model of the knee-joint[J]. *Journal of biomechanics*, 1980, 13(8): 677-685.

[14] Wang J, Li X, Huang T H, et al. Comfort-centered design of a lightweight and backdrivable knee exoskeleton[J]. *IEEE Robotics and Automation Letters*, 2018, 3(4): 4265-4272.

[15] Walker P S, Rovick J S, Robertson D. The effects of knee brace hinge design and placement on joint mechanics[J]. *Journal of biomechanics*, 1988, 21(11): 965-974.

[16] Iwaki H, Pinskerova V, Freeman M A R. Tibiofemoral movement 1: the shapes and relative movements of the femur and tibia in the unloaded cadaver knee[J]. *Journal of Bone and Joint Surgery. British Volume*, 2000, 82-B(8): 1189-1195.

[17] Zhang J, Zhu A, Li X, et al. Parallel Elastic Self-Alignment Mechanism Enhances Energy Efficiency and Reduces Misalignment in a Powered Knee Exoskeleton[J]. *IEEE Transactions on Biomedical Engineering*, 2024.

[18] Suzuki K, Mito G, Kawamoto H, et al. Intention-based walking support for paraplegia patients with robot suit HAL[J]. *Advanced Robotics*, 2007, 21(12): 1441-1469.

[19] Strausser K A, Swift T A, Zoss A B, et al. Prototype medical exoskeleton for paraplegic mobility: first experimental results[C]//*Dynamic Systems and Control Conference: Vol. 44175*. 2010: 453-458.

[20] Stienen A H, Hekman E, Van Der Helm F C, et al. Self-aligning exoskeleton axes through decoupling of joint rotations and translations[J]. *IEEE Transactions on Robotics*, 2009, 25(3): 628-633.

[21] Zhang L, Liu G, Han B, et al. Assistive devices of human knee joint: a review[J]. *Robotics and Autonomous Systems*, 2020, 125: 103394.

[22] Shiraishi Y. Functional assessment for the natural knee joints in squat activity by simulation of 2D X-ray images based on 3D CT image[J]. *Trans Jpn Soc of Mech Eng*, 2011, 77: 219.

[23] Walker P S, Kurosawa H, Rovick J S, et al. External knee joint design based on normal motion[J]. *J Rehabil Res Dev*, 1985, 22(1): 9-22.

[24] Radcliffe C W. Four-bar linkage prosthetic knee mechanisms: Kinematics, alignment and prescription criteria[J]. *Prosthetics & Orthotics International*, 1994, 18(3): 159-173.

[25] Zavatsky A B, O'Connor J. A Model of Human Knee Ligaments in the Sagittal Plane: Part 1: Response to Passive Flexion[J]. *Proceedings of the Institution of Mechanical Engineers, Part H: Journal of Engineering in Medicine*, 1992, 206(3): 125-134.

[26] Karami M, Maurice G, Andre J M. A model of exo-prosthesis of the knee optimized with respect to the physiological motion of condyles[J]. *ITBM-RBM*, 2004, 25(3): 176-184.

[27] Bertomeu J M B, Lois J M B, Guillem R B, et al. Development of a hinge compatible with the kinematics of the knee joint[J]. *Prosthetics and Orthotics International*, 2007, 31(4): 371-383.

[28] Asker A, Xie S, Dehghani-Sani A. Multi-objective optimization of force transmission quality and joint misalignment of a 5-bar knee exoskeleton[C]//*2021 IEEE/ASME international conference on advanced intelligent mechatronics (AIM)*. IEEE, 2021: 122-127.

[29] Qu X, Chu H, Liu W. Design of A Lower Limb Rehabilitation Training Robot Based on A Double Four-Bar Synchronous Motion Mechanism[C]//*International Conference on Intelligent Robotics and Applications*. Singapore: Springer Nature Singapore, 2023: 540-551.

[30] Kapsalyamov A, Hussain S, Brown N A, et al. Synthesis of a six-bar mechanism for generating knee and ankle motion trajectories using deep generative neural network[J]. *Engineering Applications of Artificial Intelligence*, 2023, 117: 105500.

[31] Xiao B, Shao Y, Zhang W. Design and optimization of single-degree-of-freedom six-bar mechanisms for knee joint of lower extremity exoskeleton robot[C]//*2019 IEEE International Conference on Robotics*

and Biomimetics (ROBIO). IEEE, 2019: 2861-2866.

[32] Sabzali H, Koochakzadeh E, Moradi A, et al. Kinematics and dynamics optimization of a novel non-circular gear-attached four-bar mechanism for knee exoskeleton robot[C]//2022 10th RSI International Conference on Robotics and Mechatronics (ICRoM). IEEE, 2022: 190-195.

[33] Sun Y, Ge W, Zheng J, et al. Design and evaluation of a prosthetic knee joint using the geared five-bar mechanism[J]. IEEE Transactions on Neural Systems and Rehabilitation Engineering, 2015, 23(6): 1031-1038.

[34] Wang G, Zhou M, Sun H, et al. Mechanism Analysis and Optimization Design of Exoskeleton Robot with Non-Circular Gear-Pentabar Mechanism[J]. Machines, 2024, 12(5): 351.

[35] Wang Z, Ge W, Zhang Y, et al. Optimization Design and Performance Analysis of a Bionic Knee Joint Based on the Geared Five-Bar Mechanism[J]. Bioengineering, 2023, 10(5): 582.

[36] Olinski M. Knee joint prototype based on cam mechanism – design and video analysis[J]. Computer Methods in Biomechanics and Biomedical Engineering, 2023, 26(14): 1691-1701.

[37] Arfaie O, Unal R. KnExo, design, development, and functional evaluation of a bio-joint shaped knee exoskeleton assisting in sit to stand[J]. Authorea Preprints, 2024.

[38] Soong R C. A new cam-geared mechanism for exact path generation[J]. Journal of Advanced Mechanical Design, Systems, and Manufacturing, 2015, 9(2): JAMDSM0020-JAMDSM0020.

[39] Kim T, Jeong M, Kong K. Bioinspired knee joint of a lower-limb exoskeleton for misalignment reduction[J]. IEEE/ASME Transactions on Mechatronics, 2021, 27(3): 1223-1232.

[40] Liu Z, Han J, Han J, et al. Design and Evaluation of a Lightweight, Ligaments-Inspired Knee Exoskeleton for Walking Assistance[J]. IEEE Robotics and Automation Letters, 2024.

[41] Wang Y, Zhang W, Shi D, et al. Design and control of an adaptive knee joint exoskeleton mechanism with buffering function[J]. Sensors, 2021, 21(24): 8390.

[42] Zhao Han, Wang Bing, Yang Yuwei, et al. Research on Adaptive Variable Stiffness Load Optimization of Knee Exoskeleton Robot [J]. High Technology Letters, 2022, 32(1): 93-100.

[43] Yang Canjun, Peng Zhenzhe, Xu Linghui, et al. Design of a Flexible Knee Joint Protective Exoskeleton and Its Walking Assistance Method [J]. Journal of Zhejiang University (Engineering Science), 2021, 55(2).

[44] Sridar S, Qiao Z, Muthukrishnan N, et al. A soft-inflatable exosuit for knee rehabilitation: Assisting swing phase during walking[J]. Frontiers in Robotics and AI, 2018, 5: 44.

[45] Fang J, Yuan J, Wang M, et al. Novel Accordion-Inspired Foldable Pneumatic Actuators for Knee Assistive Devices[J]. Soft Robotics, 2020, 7(1): 95-108.

[46] Panizzolo F A, Galiana I, Asbeck A T, et al. A biologically-inspired multi-joint soft exosuit that can reduce the energy cost of loaded walking[J]. Journal of NeuroEngineering and Rehabilitation, 2016, 13(1): 43.

[47] Di Natali C, Poliero T, Sposito M, et al. Design and evaluation of a soft assistive lower limb exoskeleton[J]. Robotica, 2019, 37(12): 2014-2034.

[48] Celebi B, Yalcin M, Patoglu V. AssistOn-Knee: A self-aligning knee exoskeleton[C]//2013 IEEE/RSJ International conference on intelligent robots and systems. IEEE, 2013: 996-1002.

[49] Choi B, Lee Y, Kim J, et al. A self-aligning knee joint for walking assistance devices[C]//2016 38th Annual International Conference of the IEEE Engineering in Medicine and Biology Society (EMBC). IEEE, 2016: 2222-2227.

[50] Sarkisian S V, Ishmael M K, Hunt G R, et al. Design, development, and validation of a self-aligning mechanism for high-torque powered knee exoskeletons[J]. IEEE Transactions on Medical Robotics and Bionics, 2020, 2(2): 248-259.

[51] A method for analyzing wearing uncertainties and enhancing motion transmission smoothness in exoskeletons and its applications for a novel passive knee exoskeleton[J]. Mechanism and Machine Theory, 2024, 197: 105648.

[52] Li G, Liang X, Lu H, et al. Development and validation of a self-aligning knee exoskeleton with hip rotation capability[J]. IEEE Transactions on Neural Systems and Rehabilitation Engineering, 2024, 32: 472-481.

[53] Choi B, Lee Y, Lee J, et al. Development of adjustable knee assist device for wearable robot based on linkage and rolling joint[C]//2019 IEEE/RSJ International Conference on Intelligent Robots and Systems (IROS). IEEE, 2019: 4043-4050.

[54] Li H, Sui D, Ju H, et al. Mechanical compliance and dynamic load isolation design of lower limb exoskeleton for locomotion assistance[J]. IEEE/ASME Transactions on Mechatronics, 2022, 27(6): 5392-5402.

[55] Yang X, Guo S, Wang P, et al. Design and Optimization Analysis of an Adaptive Knee Exoskeleton[J]. Chinese Journal of Mechanical Engineering, 2024, 37(1): 104.

[56] Wen Yaoqi, Yang Yuwei, Zu Yizhou, et al. Performance Optimization and Methodology of a Knee

*Exoskeleton Robot Donning System Considering Comfort [J]. Journal of Biomedical Engineering, 2023, 40(1): 118.*  
[57] Zhang Junhui, Pan Zhiwen, Jia Ruiheng, et al. *Optimization Method for Upper Limb Exoskeleton Master-Slave Control of Hydraulic Manipulator Based on Human-Machine Matching: CN118061156B [P]. 2024-08-23.*